Polymer 55 (2014) 6552–6560

Contents lists available at ScienceDirect

Polymer

journal homepage: www.elsevier.com/locate/polymer

Thermo-responsive brush copolymers with structure-tunable LCST and switchable surface wettability

Jin-Jin Li, Yin-Ning Zhou, Zheng-Hong Luo*

Department of Chemical Engineering, School of Chemistry and Chemical Engineering, Shanghai Jiao Tong University, Shanghai 200240, PR China

ARTICLE INFO

Article history:
Received 10 July 2014
Received in revised form
17 September 2014
Accepted 7 October 2014
Available online 22 October 2014

Keywords:
Thermo-responsive brush copolymers
Structure-tunable LCST
Thermo-responsive wettability

ABSTRACT

Thermo-responsive brush copolymers poly(methyl methacrylate (MMA)-*co*-2-(2-bromoisobutyryloxy) ethyl methacrylate (BIEM)-*graft*-(N-isopropyl-acrylamide) (NIPAAm)) were synthesized using Cu-mediated "living" radical polymerization (LRP) approach. Varied grafting densities of the brushes were obtained through adjusting backbone structure as random, gradient and block respectively. The effect of grafting densities on their thermo-responsive phase transition behaviors in aqueous solution and on surface were investigated in detail. The lower critical solution temperature (LCST) of brush copolymers in solution was adjusted as 35, 37 and 38 °C through random, gradient and block backbone structure respectively. Their structure tunable thermo-responsive phase transition in solution were further confirmed by the different micelle aggregation behaviors above LCST which monitored by transmission electron microscopy (TEM) images and dynamic light scattering (DLS). In addition, surfaces modified by the resulted brush copolymers have a temperature tunable wettability based on thermo-responsive phase transition in solid, the similar WCA variation range of three brush copolymers implies that the composition of backbone does not much affect the switchable wettability of surfaces.

1. Introduction

Stimuli-responsive brush copolymers with increasing complexities and defined three-dimensional morphologies present unusual hierarchical nano-assemblies in bulk and aqueous medium responding to the slightly external changes [1–4]. Various types of stimuli, e.g., temperature [5], pH [6,7], ionic strength [8], and light [9,10], have been imported to brush copolymers. Compared with others, temperature is a stimulus which can be uniformly adjusted. Poly(N-isopropylacrylamide) (PNIPAAm) with an easily accessible lower critical solution temperature (LCST~32 °C) in water is one of the mostly studied thermo-sensitive polymer [11,12]. Its LCST is close to the body temperature and can be easily tuned, which facilitate the applications in biological filed [13,14]. In addition, PNIPAAm or PNIPAAm-based polymers modified smart surfaces can realize the wettability transition from hydrophilic to hydrophobic over a narrow temperature range [15]. Such thermo-responsive surfaces are expected to be used in tissue engineering [16], biosensor [17], microfluidic devices [18], controllable capture and release of cancer cells [19], chromatography [20]. Therefore, PNIPAAm-based thermo-responsive brush copolymers were extensively explored [21,22].

The interactions between side chains usually exhibit a dramatic effect on the chemical properties of brush copolymers through causing the change of conformation of polymer chains [23]. Among the factors that influence steric repulsion of neighboring side chains, both the grafting density and the side chain length have been shown to own critical importance [24–32].While most earlier studies focused on the changes induced by the length of side chain. How the spatial variety of the side chain on the backbone affects the properties of brush copolymers have not been well characterized, to date. Hence, direct visual information about the influence of grafting density on the morphological behaviors of PNIPAAm brush copolymers should be provided. By the advent of controlled preparation of macromolecular brushes through "grafting from" macroinitiators based on "living" radical polymerization (LRP) technique, high grafting density and purified brush copolymers can be obtained [33]. And thus, it is convenient to prepare well controlled brush copolymers with different grafting density through direct adjusting the backbone construction [34,35].

In this study, PNIPAAm brush copolymers with different backbone composition profiles [poly(MMA-*co*-BIEM-*graft*-NIPAAm)] are prepared through "grafting from" macroinitiators with random, gradient, and block linear structures respectively using Cu-

---

* Corresponding author. Tel./fax: +86 21 54745602.
E-mail address: luozh@sjtu.edu.cn (Z.-H. Luo).

http://dx.doi.org/10.1016/j.polymer.2014.10.025
0032-3861/

mediated LRP approach. The synthesized PNIPAAm-based brush copolymers with varied grafting densities through adjusting the distribution of the side chains are used to study the temperature induced phase transition behaviors in solution and on the surface for the first time. The solution properties are analyzed by determining the LCST using UV–Vis spectra, and visualizing the morphological changes of the micelles based on the phase transition using TEM and DLS. Finally, the wettability of the as-fabricated surfaces is further investigated by temperature-controlled static water contact angle (SWCA) measurement at various temperatures.

2. Experimental

2.1. Materials

Methyl methacrylate (MMA, 99%, Sinopharm Chemical Reagent Co., Ltd. (SCRC)) was rinsed with 5 wt. % aqueous NaOH solution to remove inhibitor , dried with anhydrous $MgSO_4$ over night and distilled before use. 2-Hydroxyethyl methacrylate (HEMA, 95%, TCI (Shanghai) Development Co., Ltd.) was purified by washing an aqueous solution of monomer with hexane to remove ethylene glycol dimethacrylate, salting the monomer out of the aqueous phase by adding NaCl, drying with anhydrous $MgSO_4$, and distilling under reduced pressure. N-isopropylacrylamide (NIPAAm, 98%, Adamas) was recrystallized from a toluene/hexane solution ($v/v = 1/2$) and dried under vacuum prior to use. 4,4′-Dinonyl-2,2′-bipyridyl (dNbpy, Nanjing Chemzam Pharmtech, 99%) was recrystallized three times from ethanol. CuBr (99%, SCRC) was sequentially washed with acetic acid and methanol and dried under vacuum at 45 °C for 24 h. Tetrabutylammonium fluoride (TBAF, 1 M in tetrahydrofuran (THF), TCI (Shanghai) Development Co., Ltd.), ethyl 2-bromoisobutyrate (Eib-Br, 98%, Alfa Aesar), 2-bromoisobutyryl bromide (98%, Alfa Aesar), hexamethylated tris (2-aminothyl) amine (Me_6TREN, 99%, Alfa Aesar), copper powder (75 μm, 99%, Sigma–Aldrich) and potassium fluoride (KF, 99%, SCRC) were used as received without further purification.

2.2. Preparation of poly(MMA-co-BIEM-graft-NIPAAm)

Thermo-responsive brush copolymers with three different backbone structure were synthesized in two steps: first, random, gradient and block macroinitiators poly(MMA-*co*-BIEM) with similar average chemical composition ($F_{\mathrm{BIEM}} \approx 0.38$) were synthesized in batch or semi-batch mode. Subsequently, brush copolymers poly(MMA-*co*-BIEM-*graft*-NIPAAm) were synthesized by the “grafting from” method. The detailed copolymers preparation process in this work is described as follows (shown in Scheme 1).

2.2.1. Synthesis of poly(MMA-co-HEMA-TMS)

2-(trimethylsilyl)ethyl methacrylate (HEMA-TMS) instead of HEMA is usually used to synthesize block copolymers due to its high solubility in organic media [36]. Random copolymer and diblock copolymer were both prepared via batch Cu-mediated LRP. The typical batch procedure is as follow: toluene, monomer and catalyst system were first added into a flask, after deoxygenization, the initiator Eib-Br or PMMA-Br was added under N_2, finally the reaction was carried out at 90 °C for 7 h. The gradient copolymer was synthesized through semi-batch Cu-mediated LRP as follows: toluene, MMA and catalyst system were first added into a flask. After deoxygenization, the initiator Eib-Br was added under N_2. Synchronously, the second mixture (catalyst system and HEMA-TMS) was continuous added into the first one at a model optimized rate corresponding to targeted composition [34]. The reaction was also carried out at 90 °C for 7 h.

Poly(MMA-*co*-HEMA-TMS) with random, gradient and block composition profiles were obtained after removing copper complex via passing the polymer solutions through a neutral alumina column and precipitating in methanol. Recipes for the experimental studies were listed in Table 1.

2.2.2. Synthesis of poly(MMA-co-BIEM)

Firstly, 2 g of poly(MMA-*co*-HEMA-TMS) (containing 5.5 mmol HEMA-TMS) was dissolved in 80 mL dry THF, following by adding KF (334 mg, 5.5 mmol) and TBAF (550 μL, 0.6 mmol). The solution was stirred for 24 h at room temperature. Subsequently, triethylamine (3.0 mL, 22.0 mmol) and 2-bromoisobutyl bromide (1.5 mL, 11.0 mmol) were slowly added into the polymer solution at 0 °C. The mixture was stirred for another 24 h. The macroinitiator [poly(MMA-*co*-BIEM)] was obtained through precipitating the polymer solution into methanol.

2.2.3. Synthesis of poly(MMA-co-BIEM-graft-NIPAAm)

The brush copolymers with different backbone composition profiles were synthesized by grafting polymerization of NIPAAm monomer from random, gradient, and di-block macroinitiators [poly(MMA-*co*-BIEM)], respectively. The typical procedure was introduced as follows. Poly(MMA-*co*-BIEM) (0.025 mmol initiating sites), N,N-dimethylformamide (DMF)/2-propanol mixed solution ($v/v = 3/1$, 3 mL), copper powder (1.6 mg, 0.025 mmol), hydrazine hydrate (1.2 μL, 0.025 mmol) and Me_6TREN (6.5 μL, 0.025 mmol) were first introduced into a 25 mL Schlenk flask and stirred for 5 min. And then, NIPAAm (1.13 g, 10 mmol) dissolving in 1 mL DMF/2-propanol mixed solution ($v/v = 3/1$) was added to the flask. After three freeze–pump–thaw cycles, the polymerization was carried out at 25 °C for 4 h. The reaction mixture was diluted with $CHCl_3$ and passed through Al_2O_3 column to remove the catalyst. Finally, the brush polymer [poly(MMA-*co*-BIEM-*graft*-NIPAAm)] was obtained through pouring the concentrated solution into anhydrous ethyl ether.

2.3. Preparation of poly(MMA-co-BIEM-graft-NIPAAm) solution

5 mg brush copolymer was first dissolved in 1 mL DMF. Next, the solution was slowly added into double-distilled water (10 mL) under vigorous stirring. After dialyzing the solution against distilled water for 2 days, a 0.5 mg/mL micelle solution was obtained.

2.4. Preparation of the copolymers films

The polymer solution (3 wt% in $CHCl_3$) was spin-casted onto clean silicon wafer at 3000 rpm for 30 s, and then dried naturally for 24 h. Before use, the silicon wafers were carefully cleaned in a beaker of 10% HCl and KF solution for 24 h and followed by successive acetone, ethyl alcohol and deionized water placed in an ultrasonic bath for at least 20 min at room temperature and then dried with nitrogen stream.

2.5. Measurements

The compositions of copolymers were determined by nuclear magnetic resonance (^{1}H NMR) spectroscopy (Varian Mercury plus 400, 400 MHz) in $CDCl_3$ with tetramethylsilane (TMS) internal standard.

Molecular weights (M_n) and molecular weight distributions (M_w/M_n) of polymers were determined on a gel permeation chromatograph (GPC, Tosoh Corporation) equipped with two HLC-8320 columns (TSK gel Super AWM-H, pore size: 9 μm; 6 × 150 mm, Tosoh Corporation) and a double-path, double-flow a refractive

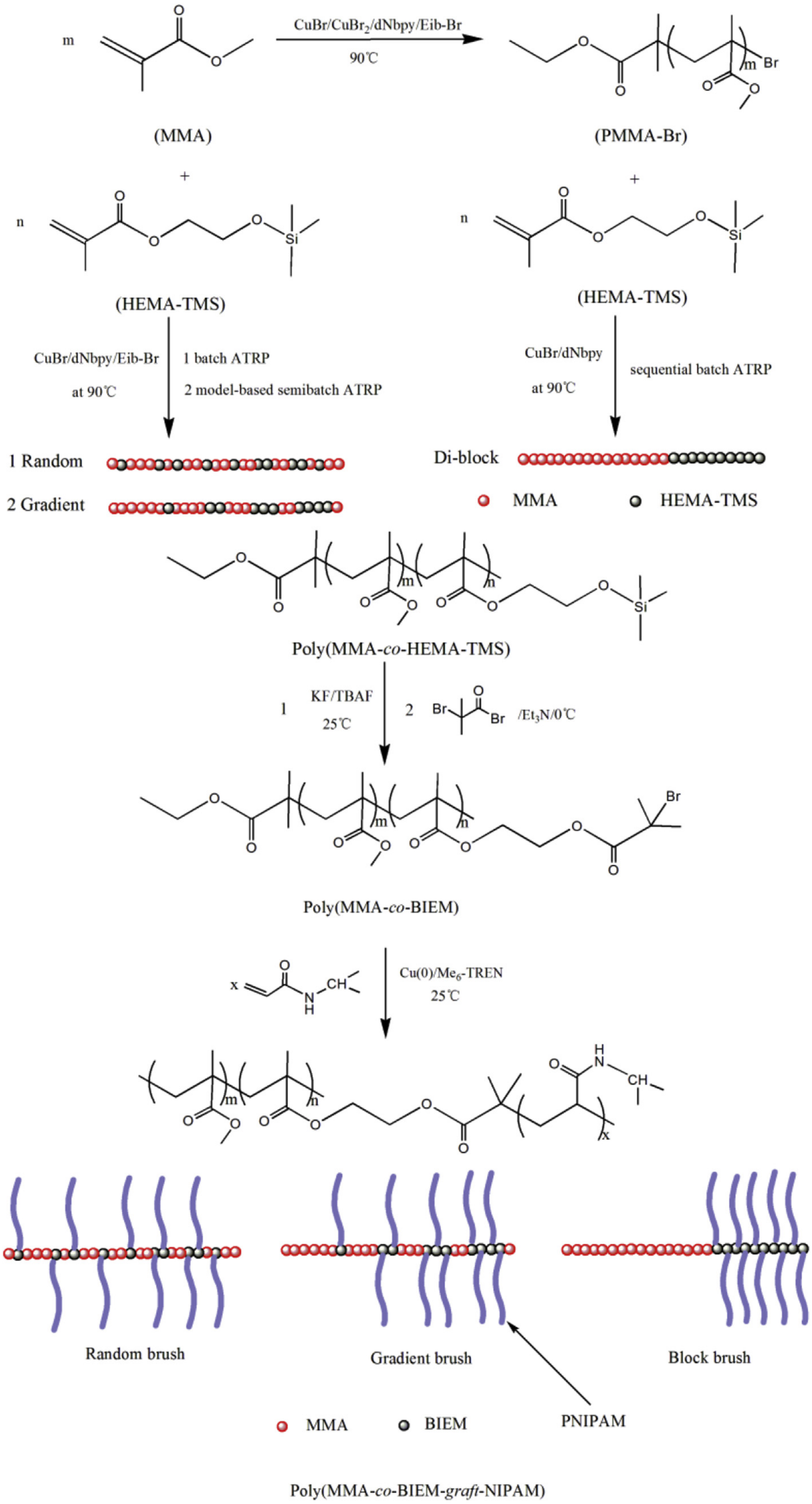

Scheme 1. Synthetic outline of poly(MMA-*co*-BIEM-*graft*-NIPAAm).

Table 1
Recipes for the experimental studies.

Expt.		MMA [mmol] ([mL])	HEMA-TMS [mmol] ([mL])	Initiator [mmol]	CuBr [mmol]	$CuBr_2$ [mmol]	dNbpy [mmol]	Solvent [mL]	V_f [mL/h]
1	r. f.	37.5(4)	36(7.5)	0.35	0.35	0.0175	0.70	5.0	
2	r. f.	37.5(4)		0.35	0.18	0.090	0.36	3.0	
	a.s.		36(7.5)		0.17	0.085	0.34	2.0	1.5
3	r. f.		36(7.5)	0.36	0.36	0.018	0.72	5.0	

where, r. f. = reactive flask, a. s. = airtight syringe.

index detector (Bryce) at 30 °C. The elution phase was DMF (0.01 mol/L LiBr, elution rate: 0.6 mL/min), and a series of poly methyl methacrylate (PMMA) were used as the conventional calibration standard.

Dynamic Light Scattering (DLS) measurements were performed on the self-assembly aqueous solutions using a ZS90 Zetasizer Nano ZS instrument (Malvern Instruments Ltd., U.K.) equipped with a 4 mW He–Ne laser ($\lambda = 633$ nm) at an angle of 90°.

The UV–vis spectra were recorded on a UV-2550 spectrophotometer (Shimadzu, Japan). UV–vis spectroscopy was used for transmission measurements on samples of 0.5 mg/mL at 500 nm. Transmission was monitored at temperature increment of 1 °C with equilibration times of 1 min.

The transmission electron microscope (TEM) images of self-assembly samples were obtained using a JEM-2100 (JEOL Ltd., Japan) TEM operated at an acceleration voltage of 200 kV. The samples were prepared by dropping the micellar solution at a given temperature onto a piece of preheated copper grid till the solvent was evaporated.

The static water contact angle (SWCA) of silicon surfaces functionalized by brush copolymers were measured using the sessile drop method on a Contact Angle Measuring Instrument (KRUSS, DSA30) at the temperatures of 25, 30, 35, 40, 45, 50, 55, 60 °C. The temperature was controlled by a Temperature Controller TC40-MK2. Deionized water droplet (5 μL) was dropped onto the samples which were blow-dried with N_2 and kept at the required temperature for 10 min.

3. Results and discussion

3.1. *Characterization of brush copolymers with different linear composition profiles*

Three linear copolymers with different initiator sites distribution and similar cumulative composition were synthesized via Cu-mediated LRP. The overall ratio of incorporated monomer in the resulting poly(MMA-*co*-HEMA-TMS) was determined using ^{1}H NMR measurement by comparing the peak area ratio of characteristic signals for PMMA (3.6 ppm, 3H, $-O-CH_3$) and P(HEMA-TMS) (4.01 ppm, 2H, $-CH_2-OCO-$; 3.76 ppm, 2H, $-CH_2-O-$; 0.14 ppm, 9H, $-Si(CH_3)_3$) in Fig. 1a. The molecular weight obtained through calculating and GPC measurements, as well as molecular weight distribution of the resulting copolymers are listed in Table 2.

The ^{1}H NMR measured cumulative profiles in Fig. 2 depict how the chemical composition changes during the reaction. One can find that the evolutions of $F_{cum,HEMA\text{-}TMS}$ with degree of polymerization are different, but ending at about 0.38. The nearly constant $F_{cum,HEMA\text{-}TMS}$ of random copolymer implies the statistically distributed composition profile along the chains. And the $F_{cum,HEMA\text{-}TMS}$ gradually increases from the beginning of polymerization to the end, showing a gradient composition profile. Without exception, the evolution of block copolymer has an abrupt step change in composition at the block joint location.

Subsequently, macroinitiators [poly(MMA-*co*-BIEM)] with different backbone structures were obtained and the ^{1}H NMR spectrum is shown in Fig. 1(b) (taking poly(MMA-*grad*-BIEM) as an example). On the spectrum, peak at 0.14 ppm ($-Si(CH_3)_3$) completely disappears because of the removal of TMS groups, new peak corresponding to methyl protons of $-C(CH_3)_2-Br$ appears at 1.97 ppm after esterification. Simultaneously, peaks at 4.01 ppm ($-CH_2-OCO-$) and 3.76 ppm ($-CH_2-O-$) shift to 4.21 ppm and 4.37 ppm, respectively. The peak at 3.60 ppm corresponding to the protons on MMA units remains unchanged. After shifting, the ratio of the characteristic peak areas at $\delta = 4.21$ ppm, at $\delta = 4.37$ ppm and at $\delta = 3.60$ ppm is 1:1:2.5 [Fig. 1(b)], which is the same as that at $\delta = 4.01$ ppm, at $\delta = 3.76$ ppm and at $\delta = 3.60$ ppm [Fig. 1(a)], indicating the 100% efficiency of esterification.

The brush copolymers [poly(MMA-*co*-BIEM-*graft*-NIPAAm)] were synthesized by Cu(0)-mediated LRP of NIPAAm monomer using poly(MMA-*co*-BIEM) as macroinitiators. As shown in Table 2, the M_ns of the obtained graft copolymers clearly increase compared with that of precursors. In a typical ^{1}H NMR spectrum of poly(MMA-*grad*-BIEM-*graft*-NIPAAm) [Fig. 1(c)], the characteristic signals at $\delta = 4.0$ ppm and $\delta = 6.0$–7.0 ppm corresponding to the methine proton of isopropyl groups and the amide proton next to the isopropyl groups of PNIPAAm, respectively, are clearly observed, which verify the successful synthesis of brush copolymers. The average repeating unit of PNIPAAm side chains can be calculated using the ratio of the peak area at $\delta = 3.6$ ppm (the characteristic signal of PMMA) to that at $\delta = 4.0$ ppm. The results are listed in Table 2.

3.2. *Structure tunable thermo-responsive phase transition behaviors*

Combining or grafting PNIPAAm with other hydrophobic polymers can increase the LCST to or slightly above the body temperature due to the hydrophobic interactions among the copolymer segments [37–41]. To determine the effect of backbone architectures on the thermo-responsive property of the brush copolymers, the turbidity of three brush copolymer micelle aqueous solutions was examined at 500 nm as a function of temperature. The LCST was defined as the specific temperature which producing a 50% decrease in transmittance [42]. As shown in Fig. 3, brush copolymer aqueous solutions become turbid as the temperature increase above LCST and all the LCSTs shift to a higher value than that of PNIPAAm (32 °C). These results possibly caused by the strengthened inter-polymer hydrophobic interaction between backbone copolymers, which can be explained through the Flory-Huggins solution theory according to the previous literature [43]. More interestingly, random, gradient and block brush copolymer micelle solutions exhibit thermo-responsive behaviors at 35 °C, 37 °C and 38 °C respectively. Compared with the previous literatures about tailoring the LCST of temperature-responsive copolymers, the improvements resulted in this work are encouraging. For example, Zhang et al. [43] improved the LCST of poly(N-isopropylacrylamide)-block-poly(lactic acid)-block-poly(N-isopropylacryl- amide) (PNIPAAm-b-PLA-b-PNIPAAm) triblock copolymers about 2.5 °C via stereocomplexation of two enantiomeric forms of PLA; Liu et al. [41] improved the LCST of copolymer from 38.2 °C to 40 °C through

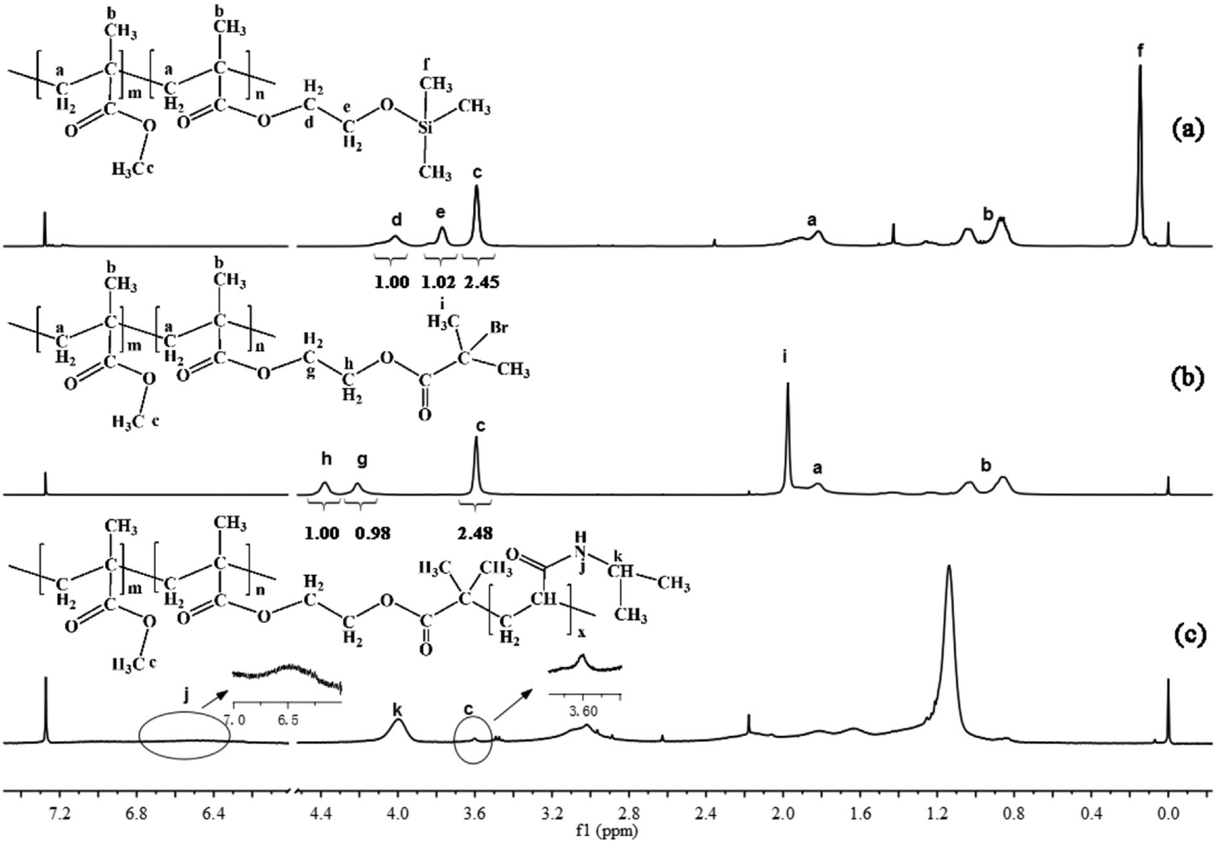

Fig. 1. ^{1}H NMR spectra of (a) poly(MMA-*grad*-HEMA-TMS), (b) poly(MMA-*grad*-BIEM), and (c) poly(MMA-*grad*-BIEM-*graft*-NIPAAm) in $CDCl_3$.

grafting cholesteryl onto functional amphiphilic poly(N-isopropylacrylamide-co-N-hydroxylmethylacryl-amide).

Furthermore, the spatial arrangement of side chains along the backbone could dramatically affect the assembly of brush polymers through changing the repulsive force among side chains [35,44]. Accordingly, we suspect that the different phase transition of brush copolymers in solutions mainly depends on the backbone structure induced inconsistent conformational changes of the micelles.

In order to confirm the above hypothesis, the thermo-responsive conformation changes of brush polymer micelles were monitored by TEM and DLS (Figs. 4–6). The TEM observation shows that, at low temperature ($T = 25$ °C), micelles containing a hydrophobic backbone core and a looped PNIPAAm corona are formed in the solution of brush copolymers. Micelles in random brush copolymer solution show irregular shape, and the diameter is approximate 35–45 nm (Fig. 4A). The diameters of sphere micelles formed by gradient and block brush copolymers are approximate 30–35 nm (Fig. 5A), and 30–40 nm (Fig. 6A) respectively. Micelle aggregation happens eventually in all brush copolymer solutions with the temperature increase above their LCST. However, the detailed aggregation processes of three brush copolymers are different (Figs. 4–6). For the random brush, the size of micelles firstly decreases in a small range as the temperature increase

Table 2
Summary of experimental results for the studied system.

Samples	Repeating unit numbers[a]			M_n[a] (KDa)	M_n[b] (KDa)	M_w/M_n[b]
	Backbone		Side chain			
	MMA	BIEM	NIPAAm			
P(MMA-*rand*-BIEM)	80	50	0	22.0	18.5	1.31
P(MMA-*grad*-BIEM)	84	49	0	22.1	19.2	1.29
P(MMA-*block*-BIEM)[c]	83	53	0	23.1	21.0	1.33
P(MMA-*rand*-BIEM-*g*-NIPAAm)	80	50	48	293.6	333.1	1.54
P(MMA-*grad*-BIEM-*g*-NIPAAm)	84	49	47	282.7	320.1	1.56
P(MMA-*block*- BIEM-*g*-NIPAAm)	83	53	44	287.0	325.2	1.57

[a] Measured by ^{1}H NMR spectroscopy.
[b] Measured by GPC using PMMA as standard performed in DMF.
[c] Prepared from PMMA-Br ($M_n = 8.0$ KDa, $M_w/M_n = 1.16$).

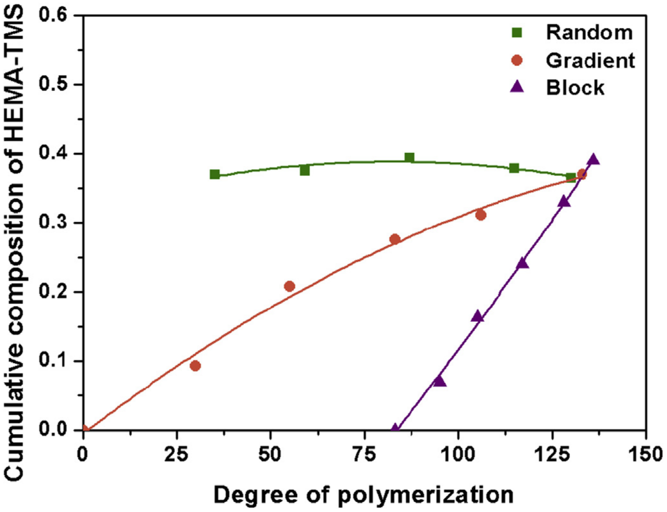

Fig. 2. Cumulative HEMA-TMS composition in poly(MMA-*co*-HEMA-TMS) as a function of the number-average chain length: the points are experimental data.

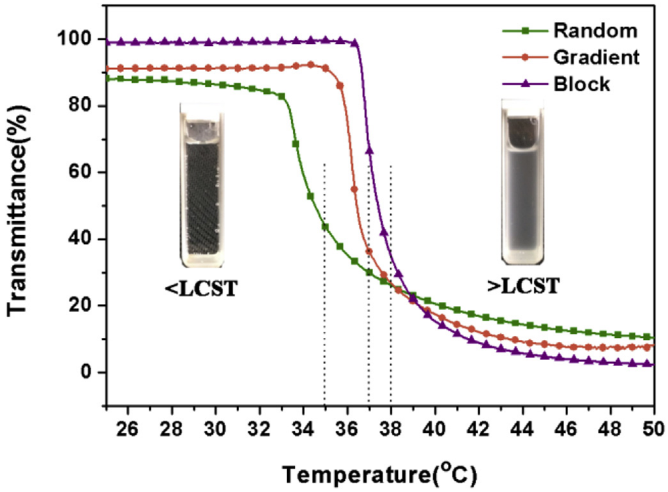

Fig. 3. Temperature dependence of the light transmittance through 0.5 mg/ml poly(-MMA-*co*-BIEM-*graft*-NIPAAm) solutions.

(Fig. 4B). When the temperature increase to 35 °C, micelles start to aggregate and irregular micelle aggregations are obtained ultimately (Fig. 4C). The DLS analyses also indicate that the size of micelles firstly decreases in a small range and then increases sharply as temperature increases above the LCST (Fig. 4D). TEM observation shows the dried aggregates under high vacuum, while DLS analysis detects the micelles with water-swollen corona. Thus, the average size of the micelles by DLS detection is much bigger than that by TEM observation.

The sphere micelles formed in the solution of gradient brush also shrink with the increase of temperature. However, the change of the size is not as obvious as the random brush due to the restrictive conformational freedom of the side chains (Fig. 5B). Then the aggregate behavior occurs at a higher temperature and the sphere micelles connect with each other in an orderly way, resulting in the aggregation with wormlike structures. This is attributed to the repulsive interaction between the micelles which is introduced by the higher density of PNIPAAm (Fig. 5C). These changes can be also observed in the DLS analysis results (Fig. 5D).

Compared with the other two brush copolymers, the sphere micelles formed by the block brush copolymer is more regular and

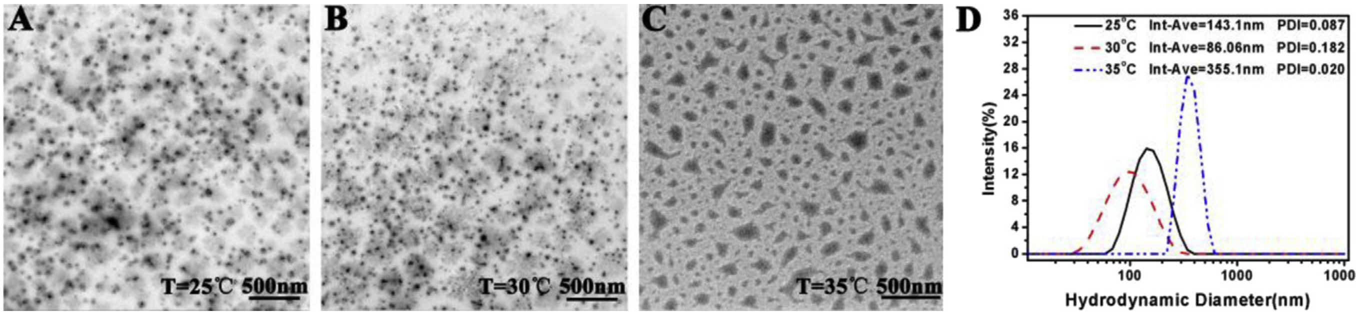

Fig. 4. TEM images of the micelles formed in random brush copolymer solution at (A) 25 °C, (B) 30 °C, (C) 35 °C. (D) DLS results of micelles at 25 °C, 30 °C and 35 °C.

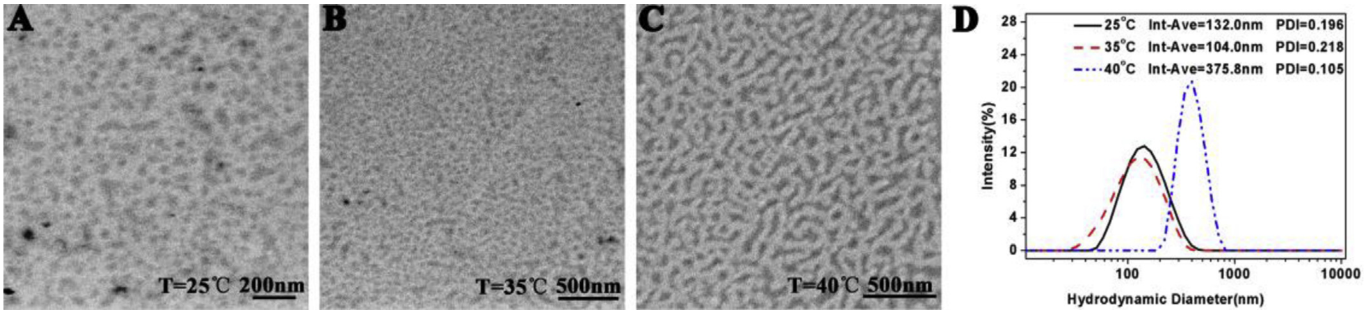

Fig. 5. TEM images of the micelles formed in gradient brush copolymer solution at (A) 25 °C, (B) 35 °C, (C) 40 °C. (D) DLS results of micelles at 25 °C, 35 °C and 40 °C.

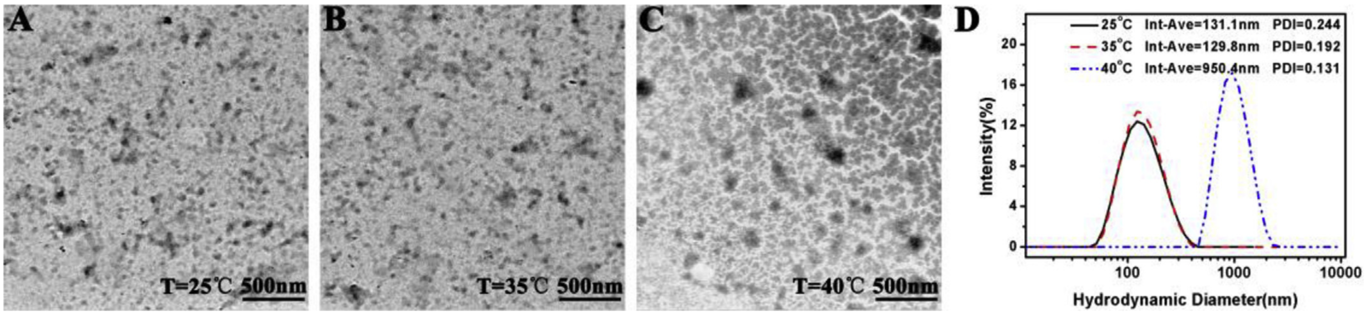

Fig. 6. TEM images of the micelles formed in block brush copolymer solution at (A) 25 °C, (B) 35 °C, (C) 40 °C. (D) DLS results of micelles at 25 °C, 35 °C and 40 °C.

there is almost no shrinkage in the corona of micelles when the temperature increase in a certain range (Fig. 6B). It is certain that the strong repulsive interaction among the denser PNIPAAm side chains within micelle leads to the above phenomenon. Simultaneously, the strongest inter-micelle repulsive interactions between PNIPAAm side chains make the compact micelle clusters eventually appear at 40 °C (Fig. 6C). The DLS analyses in Fig. 6D show the consistent variation trend with the TEM results.

The above detailed backbone structure induced different conformational changes of the micelles in solutions are schematically illustrated in Scheme 2. For random brush, grafting density remains constant along the copolymer backbone. In the aqueous solution, their backbone chains gather to form the core of the micelles through hydrophobic interactions, simultaneously, the nitrogen atoms of PNIPAAm distribute on micellar outer shell to make the micelles stably exist in solution through hydrogen bonding with water molecules. PNIPAAm segments gradually become hydrophobic as the increase of temperature, which induce progressive shrinkage of the micellar corona. When repulsive force among the side chains cannot offset the hydrophobic interactions, micelles begin to gather and the transmittance of random brush polymer solution exhibit a sharp drop (Scheme 2A).

For gradient brush, loosely grafted molecule forms on the one end and densely grafted molecule forms on the other end. Loosely grafted molecule ends are easy to insert in micelles because of their higher hydrophobicity. By contrast, densely grafted molecule ends are more inclined to distribute on the periphery of micelles, resulting in a higher NIPAAm density on the surface of micelles than random brush [35]. The increase of temperature can also weaken the hydrogen bonding between the nitrogen atoms and the water molecules. Then, the shell shrinks and the hydrodynamic radius of the micelles will decrease to some extent. However, conformational freedom of the side chains is restricted due to the higher density, resulting in a strong resistance against the further shrinkage of the corona. Therefore, the temperature of gradient polymer system for phase transition has to increase even further (Scheme 2B).

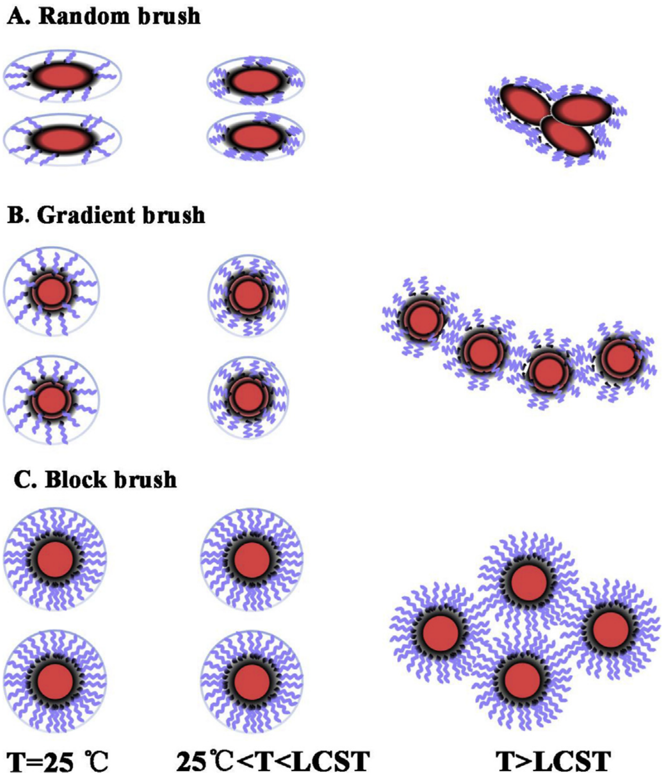

Scheme 2. Schematic illustrations of the thermo-responsive micellar behaviors in different brush copolymer aqueous solutions.

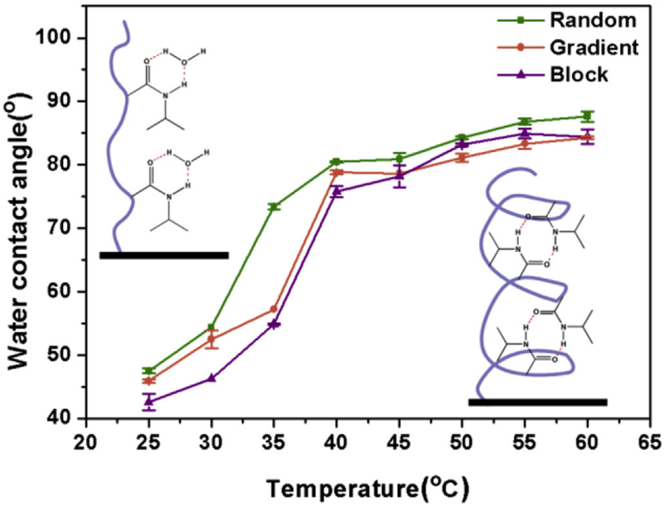

Fig. 7. Thermo-responsive wettability transition behaviors of surfaces modified by random, gradient and block brush copolymers respectively. The inset is the schematic representation of the intermolecular and intramolecular hydrogen bonding interaction for the transformation of hydrophilicity and hydrophobicity.

Due to the absence of steric hindrance from grafted side chains, the hydrophobic blocks PMMA of block brush copolymer are more likely to aggregate with each other. Sphere micelles formed by block brush with a maximum aggregation number compared to the other two brush copolymers [35]. Simultaneously, the other blocks with high grafted density bring out the strongest repulsive interactions among the side chains, making the shrinkage of micelles not so apparent when the temperature increases. Therefore, the micelles formed by block brush copolymers with the highest grafting density can stable exist in a broad temperature range (Scheme 2C).

As a whole, the PNIPAAm-based brush copolymers possess a higher LCST than that of PNIPAAm (32 °C), which is more close to the body temperature. This result will benefit their applications in biological filed. What is even more interesting is that the LCST of brush copolymers can be adjusted as 35, 37 and 38 °C through the random, gradient and block backbone structure, respectively. Their structure tunable thermo-responsive phase transition behaviors confirm the relationship between the architecture and the functional properties, and also provide valuable guidance for designing copolymers with unique properties.

3.3. *Thermo-responsive surface wettability*

In addition to the thermo-sensitive in solutions, PNIPAAm-based polymers also have thermo-responsibility in solid. The wettability of surface modified by them can transfer from hydrophilic to hydrophobic at temperature below or above LCST. As another type of thermo-responsive behavior, the influence of backbone structure on the temperature-responsive wettability of surface modified by brush copolymers was studied here.

Silicon wafers were modified by random, gradient and block brush copolymers, respectively. The wettability transition behaviors of the modified surfaces were investigated using temperature-controlled SWCA measurement from 25 to 60 °C. Results in Fig. 7 show that, in all cases, the WCA of surfaces first increases gradually from 45 to 55° when temperature below 35 °C. After a sharply increase from 55 to 80° in a relative narrow temperature range,

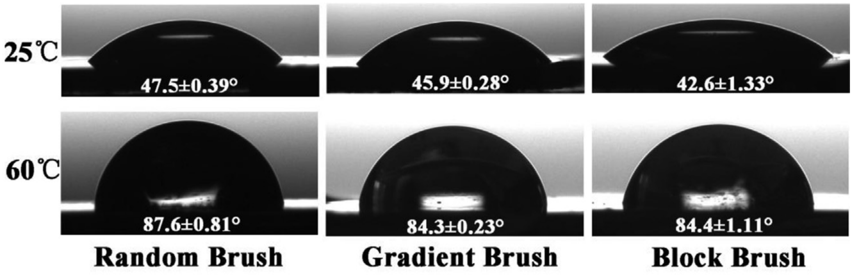

Fig. 8. The static WCA images of surfaces modified by random, gradient and block brush copolymers at 25 °C and 60 °C respectively.

their WCA values reach to a stable level. (SWCA images at start and end point temperatures are presented in Fig. 8) However, the inflection point temperatures for the three brush copolymers are little difference (all in the range of 35–40 °C), which is inconsistent with the above investigation results in the solution. This temperature-induced switchable wettability can be explained by the competition between intermolecular and intramolecular hydrogen bonding [15]. At temperatures below the LCST, the intermolecular hydrogen bonding between the PNIPAAm chains and water molecules is the dominant interaction. The extended PNIPAAm chains contribute to the hydrophilicity of brush copolymer modified surfaces. As temperature increase above LCST, the main interaction force is replaced by the hydrogen bonding between C═O and N–H groups in PNIPAAm chains. The collapsed PNIPAAm chains prevent C═O and N–H groups from interacting with water molecules, which makes the surfaces exhibit hydrophobicity at high temperatures. The graphic demonstration is present in insets of Fig. 7.

Above results confirm that surfaces modified by the resulted brush copolymers have a temperature tunable wettability, and the variations of SWCA are all about 35° when the temperature increases from 25 to 60 °C. The similar variation range implies that the composition of backbone does not much affect the wettability of surfaces modified by brush copolymers at temperature below or above LCST. We hold that thermo-responsive wettability of these surfaces is a macroscopic property which mainly depends on the quantity of NIPAAm, not on their microcosmic structure. In addition, considering the importance of the reversibility in application, the repeatability of smart surfaces was investigated. The results presented in Fig. 9 illustrate that all the smart surfaces undergo a stable reversible thermal responsive wettability by adjusting the applied temperature below and above LCST. These results provide guidance for the preparation of thermo-responsive smart surface, and the easygoing structure should be selected to meet the request and minimize the costs.

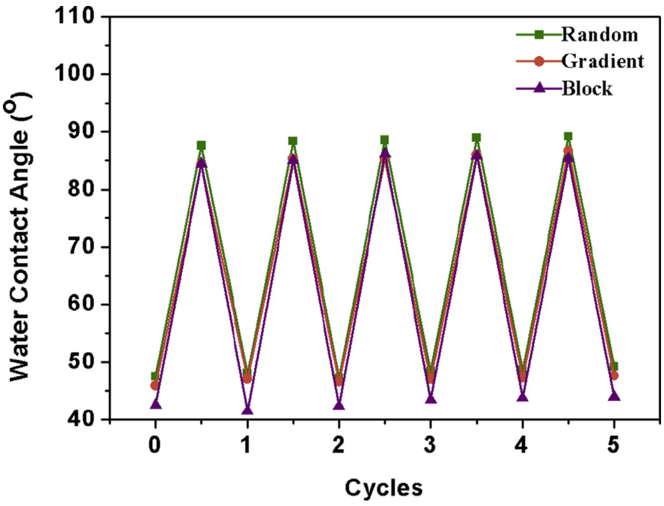

Fig. 9. Reversible static WCA transition of the surfaces modified by random, gradient and block brush copolymers respectively between 25 °C (<LCST) and 60 °C (>LCST).

4. Conclusions

It is important to understand what effects of the grafting density on the thermo-responsive properties of PNIPAAm brush copolymers. In this paper, we for the first time synthesized brush copolymers [poly(MMA-*co*-BIEM-*graft*-NIPAAm)] with varied grafting densities through adjusting the distribution of side chains based on random, gradient and block backbone structure. Particular attentions were focused on their LCST-type phase transition behaviors in aqueous solution. UV–Vis spectra monitored results showed that the LCST of random, gradient and block brush copolymer micelle solutions at 35 °C, 37 °C and 38 °C respectively.

Conformational transitions of their micelles were demonstrated by TEM images and DLS results: the onset temperature of the micellar aggregation increases according to the order from random, gradient to block brush. What is more, their aggregations formed at the LCST present irregular, wormlike and compact cluster morphologies, respectively. These results clearly confirm that the unique phase transition behaviors of three brush copolymers dependent on the grafting density are attributed to their different backbone structures.

Additionally, we modified the silicon wafers using the resulting random, gradient and block brush copolymers respectively. These thermo-responsive surfaces have a temperature tunable wettability, and the SWCA can change about 35° when the temperature increases from 25 to 60 °C. Their SWCA values at start and end points do not present apparent differences. It can be summarized that the microcosmic structure of the molecules does not much affect the macroscopic phase transition behaviors on the surface.

Acknowledgments

The authors thank the National Natural Science Foundation of China (No. 21276213), the Research Fund for the Doctoral Program of Higher Education (No. 20130073110077) and the National High Technology Research and Development Program of China (No. 2013AA032302) for supporting this work.

References

[1] Lord SJ, Sheiko SS, LaRue I, Lee H-I, Matyjaszewski K. Macromolecules 2004;37:4235–40.
[2] Boyce JR, Shirvanyants D, Sheiko SS, Ivanov DA, Qin S, Borner H, et al. Langmuir 2004;20:6005–11.
[3] Li Z, Ma J, Cheng C, Zhang K, Wooley KL. Macromolecules 2010;43:1182–4.
[4] Xia Y, Olsen BD, Kornfield JA, Grubbs RH. J Am Chem Soc 2009;131:18525–32.
[5] Li X, ShamsiJazeyi H, Pesek SL, Agrawal A, Hammouda B, Verduzco R. Soft Matter 2014;10:2008–15.
[6] Liu WY, Liu YJ, Zeng GS, Liu RG, Huang Y. Polymer 2012;53:1005–14.

[7] Shi Q, Su YL, Ning X, Chen WJ, Peng JM, Jiang ZY. J Membr Sci 2010;347:62–8.
[8] Liu XB, Luo SK, Ye J, Wu C. Macromolecules 2012;45:4830–8.
[9] Zhou YN, Li JJ, Zhang Q, Luo ZH. AIChE J 2014. http://dx.doi.org/10.1002/aic.14602.
[10] Zhou YN, Zhang Q, Luo ZH. Langmuir 2014;30:1489–99.
[11] Otake K, Inomata H, Konno M, Saito S. Macromolecules 1990;23:283–9.
[12] Kubota K, Fujishige S, Ando I. J Phys Chem 1990;94:5154–8.
[13] Kawano T, Niidome Y, Mori T, Katayama Y, Niidome T. Bioconjug Chem 2009;20:209–12.
[14] Shen Y, Kuang M, Shen Z, Nieberle J, Duan H, Frey H. Angew Chem Int Ed 2008;47:2227–30.
[15] Sun TL, Wang GJ, Feng L, Liu BQ, Ma YM, Jiang L, et al. Angew Chem Int Ed 2004;43:357–60.
[16] Tang Z, Akiyama Y, Okano T. Polymers 2012;4:1478–98.
[17] Yin Z, Zhang J, Jiang L, Zhu J. J Phys Chem C 2009;113:16104–9.
[18] Hou X, Yang F, Li L, Song Y, Jiang L, Zhu D. J Am Chem Soc 2010;132:11736–42.
[19] Liu H, Liu X, Meng J, Zhang P, Yang G, Su B, et al. Adv Mater 2013;25:922–7.
[20] Kanazawa H, Okano T. J Chromatogr A 2011;1218:8738–47.
[21] Li C, Gunari N, Fischer K, Janshoff A, Schmidt M. Angew Chem Int Ed 2004;43:1101–4.
[22] Balamurugan SS, Bantchev GB, Yang Y, McCarley RL. Angew Chem Int Ed 2005;44:4872–6.
[23] Xu Y, Bolisetty S, Ballauff M, Müller AHE. J Am Chem Soc 2009;131:1640–1.
[24] Balamurugan S, Mendez S, Balamurugan SS, O'Brien MJ, López GP. Langmuir 2003;19:2545–9.
[25] Yim H, Kent MS, Huber DL, Satija S, Majewski J, Smith GS. Macromolecules 2003;36:5244–51.
[26] Yim H, Kent MS, Mendez S, Balamurugan SS, Balamurugan S, López GP, et al. Macromolecules 2004;37:1994–7.
[27] Yim H, Kent MS, Satija S, Mendez S, Balamurugan SS, Balamurugan S, et al. J Polym Sci Part B 2004;42:3302–10.
[28] Yim H, Kent MS, Mendez S, López GP, Satija S, Seo Y. Macromolecules 2006;39:3420–6.
[29] Yim H, Kent MS, Satija S, Mendez S, Balamurugan SS, Balamurugan S, et al. Phys Rev E 2005;72:051801.
[30] Plunkett KN, Zhu X, Moore JS, Leckband D. Langmuir 2006;22:4259–66.
[31] Zhu X, Yan C, Winnik FM, Leckband D. Langmuir 2007;23:162–9.
[32] Malham IB, Bureau L. Langmuir 2010;26:4762–8.
[33] Lee H, Pietrasik J, Sheikoc SS, Matyjaszewskid K. Prog Polym Sci 2010;35:24–44.
[34] Zhou YN, Li JJ, Luo ZH. J Polym Sci Part A Polym Chem 2012;50:3052–66.
[35] Li JJ, Zhou YN, Luo ZH. Soft Matter 2012;8:11051–61.
[36] Beers KL, Boo S, Gaynor SG, Matyjaszewski K. Macromolecules 1999;32:5772–6.
[37] Schild HG, Tirrell DA. Langmuir 1991;7:1319–24.
[38] Gupta B, Kumari M, Ikram S. J Polym Res 2013;20:95–100.
[39] Tabatabaei Rezaei SJ, Nabid MR, Niknejad H, Entezami AA. Polymer 2012;53:3485–97.
[40] Wenceslau AC, dos Santos FG, Ramos ÃrRF, Nakamura CV, Rubira AF, Muniz EC. Mater Sci Eng C 2012;32:1259–65.
[41] Liu XM, Pramoda KP, Yang YY, Chow SY, He CB. Biomaterials 2004;25:2619–28.
[42] Li ST, Su Y, Dan MH, Zhang WQ. Polym Chem 2014;5:1219–28.
[43] Zhang X, Tan BH, He C. Macromol Rapid Commun 2013;34:1761–6.
[44] Li JJ, Luo ZH. Ind Eng Chem Res 2014;53:1900–8.